IRIS - Archivio Istituzionale dell'Università degli Studi di Sassari

Assessing Climate Change Impacts on Wildfire Exposure in Mediterranean Areas

Questa è la versione Post print del seguente articolo:

Original
Assessing Climate Change Impacts on Wildfire Exposure in Mediterranean Areas / Lozano, O.M., Salis, M., Ager, A.A., Arca, B., Alcasena, F.J., Monteiro, A.T., Finney, M.A., DEL GIUDICE, L., Scoccimarro, E., Spano, D.E.I.. - In: RISK ANALYSIS. - ISSN 0272-4332. - (2017). [10.1111/risa.12739]

Availability:
This version is available at: 11388/182241 since: 2021-03-02T12:00:17Z

Publisher:

Published
DOI:10.1111/risa.12739

Terms of use:

Chiunque può accedere liberamente al full text dei lavori resi disponibili come “Open Access”.

Publisher copyright

note finali coverpage

(Article begins on next page)

22 October 2026

Assessing climate change impacts on wildfire exposure in Mediterranean areas

Abstract

We used simulation modeling to assess potential climate change impacts on wildfire exposure in Italy and Corsica (France). Weather data were obtained from a regional climate model for the period 1981-2070 using the IPCC A1B emissions scenario. Wildfire simulations were performed with the MTT fire spread algorithm using predicted fuel moisture, wind speed, and wind direction to simulate expected changes in weather for three climatic periods (1981-2010, 2011-2040, and 2041-2070). Overall, the wildfire simulations showed very slight changes in flame length, while other outputs such as burn probability and fire size increased significantly in the second future period (2041-2070), especially in southern portion of the study area. The projected changes fuel moisture could result in a lengthening of the fire season for the entire study area. This work represents the first application in Europe of a methodology based on high resolution (250 m) landscape wildfire modeling to assess potential impacts of climate changes on wildfire exposure at a national scale. The findings can provide information and support in wildfire management planning and risk mitigation activities.

Keywords: fire exposure, climate change, MTT algorithm, Mediterranean areas, burn probability

1. INTRODUCTION

Wildfires pose a growing threat to ecosystems[1,2] worldwide and are frequently responsible for human casualties and substantial economic losses.[3] The occurrence of wildland fires in the Mediterranean area is mainly related to human activities[4,5], whereas area burned is dependent on many factors such as climate and weather, topography, vegetation and land use, urban sprawl and fire policies.[6,7] A number of studies have highlighted that climate and weather conditions are key factors to understand the fire spread and behavior, and directly affect spatiotemporal patterns in wildfire exposure and risk.[8–11] It is widely recognized that wildfire risk and exposure could be exacerbated by climate change. [12–20] According to the most recent Intergovernmental Panel on Climate Change (IPCC) report,[21] temperatures in southern Europe are expected to increase resulting in more frequent heat waves and droughts.[22–24] Fire activity is expected to increase in terms of both area burned and fire occurrence, although climate change impacts will be variable around the region.[12,14–18,25] However, most studies investigating climate change effects on wildfires are based on coarse scale (> 1km grid data) and therefore did not capture the local drivers of fire behavior and risk (e.g., fuels, weather, topography). For instance, previous studies on future fire risk and danger in the Mediterranean basin used coarse scale fire danger indices such as the Canadian Forest Fire Weather Index (FWI)[26] or statistical models of climate and vegetation [16,18,27–31] The fine scale patterns in fire behavior are important from a risk standpoint, and can be assessed with a number of innovative approaches for estimating and mapping wildfire risk and exposure developed in the last decade. [5,32–36] These approaches use quantitative wildfire risk assessment [34] and employ a number of relatively new large fire modelling systems.

Wildfire risk assessment includes two main factors: fire behavior probabilities and fire effects. In this paper, we focused on the first component, also called exposure analysis, which is based on the estimation of the potential wildfire intensity and on the burn probability.[37] Fire spread modeling is a necessary component for wildfire exposure assessment.[38] Landscape fire spread and behavior models such as FSim,[39] FlamMap[40] and its command line version Randig allow simulating thousands fires and generating burn probability and intensity maps based on the MTT algorithm.[41] The models have been tested and applied in a number of fire systems in the United States, Canada, Portugal, and the Mediterranean basin.[41–48] However, these models have not been fully leveraged

However, only few works in relatively small areas have been carried to analyze the potential future impacts of climate change on wildfire behavior and spread.[49–51] For instance, Arca *et al*.[49] performed fire simulations for Sardinia, Italy (24,000 km^2) to assess the impact of future (2070-2100) climate changes on spatial variations of burn probability and intensity. Mitsopoulos *et al*.[50] analyzed climate change impacts (from 1991 to 2100) on fire intensity and probability using the MTT algorithm, for an area of about 100 km^2 in Greece. More recently, Kalabodikis *et al*.[51] combined future climate data and the MTT algorithm to assess variations on burn probabilities, fire size and intensity in Messinia, Greece (3,000 km^2).

In this study we apply fine scale simulation modeling to assess the impact of climate change on fire exposure at a national scale (covering a total area of about 310,000 km^2) using a wildfire modeling approach based on the Minimum Travel Time algorithm. This work demonstrates the feasibility of the overall approach for assessing future climate change impacts on fire exposure (250 m) while considering fine scale risk factors (e.g., topography,

fuels) that influence landscape wildfire spread and behavior. The methodology and results contribute to local mapping of climate induced changes in fire regimes that can help fire managers respond to potential increased risk with improved management guidelines, risk mitigation and prevention policies.

2. METHODS

2.1. Study area

The study area is located in the Euro-Mediterranean region, and consists of the entire country of Italy as well as the French island of Corsica (Fig. 1). It is located between 35° 29’ and 47° 05’ N latitude and 8° 13’ and 18° 31’ E longitude, and covers about 310,000 km^2.

To ensure reasonable computational times for both climate change analysis and wildfire modeling phases, the study area was divided into the following seven subareas (Fig. 1, Table II): Northwest Italy (NW), Northeast Italy (NE), Central Italy (CI), South Italy (SI), Sicily (SC), Sardinia (SA) and Corsica (CO). The general criteria for the division into subareas were based on administrative limits (using provincial boundaries), climate and wildfire history.

The two main mountain ranges of the Italic peninsula are the Alps, as natural northern border, and the Apennine Mountains, which cross Italy from North to South (Fig. 2a). Flat areas are mainly concentrated in coastal zones and in the Po river area. According to the updated Köppen-Geiger climate classification (Fig. 2b)[52], the most of the study area is characterized by a temperate climate (87.5% of the total area). The semi-arid climate can only be found in a small area on the southern coast. Cold climate types without dry season can be found in the Alps, whereas the highest zones are characterized by polar climate. The vegetation

distribution within the study area is not uniform (Fig. 2c).[53] The most extended vegetation type is "grasslands" (Table I),[53] mostly situated in flat areas. Forests are mainly concentrated in hilly and mountain areas. Although shrublands (Mediterranean maquis and garrigue) represent less than 10% of the total study area, some regions like Sardinia and Corsica are mainly covered by this vegetation type. Vineyards and orchards are concentrated in some areas as the eastern areas of southern Italy and in Sicily, whereas herbaceous pastures are scattered along hills and mountains.

2.2. Input data for fire simulations

2.2.1. Topography and fuels data

We obtained information on fuels and topography to produce a landscape file, as required by RANDIG, the command line version of FlamMap used for the wildfire simulations in the study. The landscape file is composed by eight layers: elevation, slope, aspect, fuel models and canopy cover, canopy bulk density, canopy base height, and stand height. All layers included in the landscape file were set at 250m resolution in UTM projection (WGS84 datum).

Input data for elevation, aspect and slope layers were obtained from digital elevation data (90 m resolution)[54] which was resampled by bilinear interpolation to 250 m resolution. To define fuel type and canopy cover layers, we reclassified the Corine land cover map of 2006 (250 m resolution)[53] following the methodology proposed by Salis *et al*.[45] From the original 44 Corine land cover categories present in the study area, 14 main fuel types were defined (Table I, Fig. 2c). Standard[55,56] or custom fuel models were attributed to each fuel type of the study area (Table I). The custom fuel models were developed as part of previous

wildfire researches[45,57] and were applied to shrubland vegetation (Mediterranean maquis and garrigue). To each fuel model, a canopy cover class was also assigned: we used the class 4 (75-100% of canopy cover) for all pixels identified as “Forests” (coniferous, broadleaf and mixed forests), while we used the class 1 (1-25% of canopy cover) for the cells classified as “Mediterranean maquis”. The canopy fuel layers (canopy bulk density, canopy base height and stand height) were finally built using average values derived from the Italian Inventory of Forests and Forest Carbon Sinks.[58]

2.2.2. Climate projections

The CMCC-CLM climate dataset associated to the A1B IPCC emissions scenario[59] was used to obtain daily data on air temperature at 2 m, rainfall, relative humidity, wind speed and direction at 12:00 UTC for the period 1981-2070. Although we used CMIP3 data, according to the IPCC[60] the differences between CMIP3 and CMIP5 models in climate projections are quite limited. The climate projections were produced by the Euro-Mediterranean Center on Climate Change (CMCC) within the FUME project (FP7/2007–2013, Grant Agreement 243888) using the CMCC-CLM regional climate model.[61] This regional model was implemented over the Euro-Mediterranean area with boundary conditions from the CMCC-MED GCM model.[62,63] The CMCC-CLM model is a climate version of the regional COSMO model,[64] an operational non-hydrostatic mesoscale weather forecast model developed by the German Weather Service, which has been updated by the CLM-Community to develop also climatic applications. The climate simulations have been performed for the period 1981-2070 following the IPCC 20C3M protocol for the 20th century part of the

integration and the A1B scenario for the 21st century. The climate dataset presents a spatial and temporal resolution of 14 km and 6 hours, respectively, thus providing a good representation of the topography for the entire Mediterranean region and contributing to accurately represent weather conditions. Climate data have been split in three 30-year periods: one used as baseline period (1981-2010), and two as future periods (2011-2040 and 2041-2070).

2.2.3. Wind and fuel moisture for fire simulations

Daily conditions at noon of both wind direction and speed and fuel moisture content for the period 1981-2070 were derived using the climate dataset described above. In detail, wind variables were created from *U* (East-West) and *V* (North-South) wind components. The frequency of each combination of wind speed and direction values (Annex 1) was calculated for each subarea considering the three 30-year periods. Dead and live fuel moisture were estimated by using the Fine Fuel Moisture (FFMC) and Drought (DC) codes of the FWI as indicators. Both codes have been shown to be good estimators of dead and live surface fuel moisture in previous works.[28,65,66] To estimate fuel moisture conditions, for each subarea and each 30-year period, we first calculated the 25th, 50th, 75th, 90th, 95th and 97th percentile of FFMC and DC daily values for each pixel. As a result, 18 raster layers for each moisture code were produced (6 percentiles x 3 periods), which summarized FFMC and DC values for each pixel of the study area. Then, mean values of FFMC and DC of each percentile (raster layer) were calculated within each subarea. Secondly, FFMC and DC values above the Sardinian 75th percentile, considering the baseline as reference, were labeled as ‘moderate’, ‘dry’, ‘very

dry' or 'extreme' moisture categories, as reported in Table III. We associated to the abovementioned categories specific fuel moisture conditions (Table III) which were used to run the simulations. Finally, for each 30-year period and each subarea, we calculated the percentage of days corresponding to the four fuel moisture categories (moderate, dry, very dry and extreme).

We used Sardinia as a reference for the entire study area since the relationships among weather conditions, FWI codes and fuel moisture content were reported in previous works in this area, based on large amounts of field data.[28,67–70] We focused our attention on data above the 75th percentile because this threshold characterizes the driest fuel moisture conditions, which correspond to the fire season periods.

In conclusion, these analyses allowed to create frequency distributions of wind speed and direction (4 wind speed values x 8 wind directions, Annex 1) and fuel moisture conditions (moderate, dry, very dry and extreme, Annex 2) for each subarea and 30-year period, which were used as input data for the fire spread simulations.

2.2.4. Fire occurrence database

For the study area, we used the wildfire database from 1990 to 2008 provided by the JRC (Joint Research Center), which contains the total fire number and area burned per month at province level (European code NUTS3, Fig. 3). The spatial distribution of fire ignition points was produced by randomly assigning ignition coordinates within the province boundaries according to the mean annual number of fires at province level (Fig. 3a). This approach was

performed in a GIS environment and allowed to locate random fire ignitions only in burnable areas, thus excluding unburnable fuels.

We then built an ignition probability grid by smoothing the fire ignition data using the inverse distance weighting algorithm (ArcMap Spatial Analyst toolbox, ESRI Inc.), with a search distance of 5000 m. This grid was used as input for the fire spread modeling exercise.

2.3. Wildfire simulations

Simulations were performed using the minimum travel time (MTT)[71] fire spread algorithm, as implemented in RANDIG. This command line version of FlamMap allows simulating a large amount of wildfires according to a given ignition density grid. Although each single event is simulated under constant weather conditions, the fire simulations can be informed considering given frequency distributions of wind speed, wind direction and fuel moisture. This allowed us to compare the effects of the different climate conditions on the simulation outputs, for each subarea and 30-year period. RANDIG is appropriate to model short-duration single-day burn periods (e.g., 10 hours, as used in this study), such as the majority of fires in the Mediterranean Basin, while this approach could have more limitations in areas characterized by multi-day large fire events, as for instance forests in northern United States and Canada.[72] No suppression efforts were assumed for the simulations. Surface fire spread is predicted by Rothermel's equation[73] and crown fire initiation is evaluated according to Van Wagner model[74] as implemented by Scott and Reinhardt.[75]

As previously explained, the input data for the simulations were produced at 250 m resolution; the outputs were also produced at 250 m resolution.

Within each subarea, fuel moisture conditions and wind speed and direction for each event simulation were sampled from the distributions corresponding to each 30-years period, as described above. Wind fields at 250 m resolution were produced running the mass-consistent model WindNinja.[76,77] Furthermore, fire ignition locations were determined for each subarea from the ignition probability grid (as described in 'Input data'): this allowed for taking into account the historical spatial patterns of fire occurrence at provincial level. During a single fire event simulation, fuel moisture, and wind fields were hold constant.

Overall, we simulated 620,000 fire events in the entire study area for each 30-year period (a total of 1,875,000), corresponding to an average of 2 fire ignitions per square kilometer. This number of simulations resulted in more than 78% of pixels burned at least once and that the total area burned was about 10 times the entire study area. All wildfires were simulated considering a spread duration of 10 hours. We used a fixed fire spread duration of 10 hours since: 1) previous methodologies for fire risk assessment based on fire spread models contemplated the use of fixed burn periods;[72] 2) a fixed fire spread duration for all study areas and periods ensured that the differences in wildfire exposure (burn probability, fire size, etc.) were only related to climate effects and not to differences in fire duration; and 3) 10 hours is a common duration of large fires in the Mediterranean basin.[46,68]

2.4. Characterizing wildfire exposure

The exposure analysis is a part of the risk analysis and quantifies the exposure to risk factors (fire likelihood and intensity).[38]

To characterize wildfire exposure, we analyzed and processed RANDIG outputs, namely burn probability, conditional flame length and fire size, and we also calculated other specific indices such as fire potential index, high flame length burn probability and high flame length probability.

The burn probability (BP) is the probability that a pixel burns given a single fire occurrence in the study area:

$$BP = \frac{B}{n}$$

where B is the number of times a pixel burns and n is the total number of fires simulated.

Additionally, the FLP output file (Flame Length Probability) of RANDIG reports the conditional probability by twenty flame length categories of 0.5-m intervals, for each pixel of the study area. Fire intensity is calculated based on the fire spread rate predicted by the MTT algorithm and depends on the major direction of spread (i.e., heading, flanking or backing fire) in relation to the direction in which the fire encounters a pixel, slope and aspect. RANDIG converts fireline intensity (*FLI*, kW m^{-1}) to flame length (*FL*, m) using the reformulation in SI units[78] of the Byram's equation:[79]

$$FL = 0.0775 \cdot FLI^{0.46}$$

The flame length distribution provided by the FLP output is used to calculate the conditional flame length (CFL), which is the weighted mean of the different FL generated from the multiple fires burning each pixel:

$$CFL = \sum_{i=1}^{20} \frac{BP_i}{BP} \cdot FL_i$$

where FL_i is the flame length midpoint of the ith category, BP_i is the probability that the pixel burns at a fire intensity i and BP is the burn probability for the pixel.

Another output of RANDIG is the Fire Size (FS, ha) list, which indicates the size of the fire originated by each ignition point. The FS grid for the study areas was produced from the FS list and using the inverse distant weighting tool (ArcMap Spatial Analyst) with a search distance of 2500 m.

FS grid and historical ignition probability grid were then combined to calculate a specific index that we called fire potential index (FPI):[45]

$$FPI = FS \cdot IP$$

where FS is the mean fire size for all fires that originated from a given pixel and IP is the historical ignition probability. High FPI values indicate elevated likelihood of having fire ignitions able to generate large fires.

Furthermore, we calculated the High Flame Length Burn Probability (HFLBP) index, which is the probability that a pixel burns with flame length greater than 2.5 m, given one ignition within the study area:

$$HFLBP = \sum_{i=6}^{20} FLP_i \cdot BP$$

Finally, the High Flame Length Probability (HFLP) index was calculated. This index represents the probability that a pixel burns with flame length greater than 2.5 m, without making reference to the BP value of the pixel:

$$HFLP = \sum_{i=6}^{20} FLP_i$$

In few words, HFLP is the probability a pixel will burn at high flame length, considering only the fires burning that pixel. This index, in addition to the HFLBP, provides quantitative information about the probability of high fire intensity when the pixel burns.

2.5. Statistical analysis

The differences between baseline and future periods in terms of wind, fuel moisture and fire exposure indicators were evaluated by calculating the relative difference between mean values; the analysis was replicated for each subarea (Fig. 4). To assess differences in fire exposure, a One-way analysis of variance (ANOVA), performed by the general linear models method and followed by the post-hoc Student-Newman-Keuls test, was used to measure the significance of differences between mean values of the fire exposure indicators (BP, CFL, FS, FPI, HFLP and HFLBP) for each period and subarea.[80] A *p*-value of 0.01 was used as level of significance for comparisons among means. Statistical analyses were performed with R software (R Development Core Team, 2013).[81]

3. RESULTS

3.1. Overview of the projected changes in weather variables

The climate projections highlighted an increase in temperatures for the entire study area, and a decrease in relative humidity and rainfall (data not shown). Moreover, wind speed is expected to decrease in terms of average values as well as in terms of frequency of days with strong winds, particularly in northern Italy (Fig. 4, Annex 1). No relevant variations were observed for wind direction. In the following sections, changes in wind speed and direction

and fuel moisture are described in detail since these variables affect directly fire spread modeling.

3.1.1. Changes in wind speed and direction

Referring to the baseline period, the subareas with the highest incidence of the highest wind speed (21-30 and >30 km h^{-1}) were Sardinia and Sicily, followed by South Italy, Corsica and, to a lower extent, Central Italy (Annex 1). On the contrary, the subareas with high frequencies of lower wind speed days (0-10 km h^{-1}) were Northwest Italy and Northeast Italy. With respect to the variation throughout the future periods (Fig. 4, Annex 1), the general trend was an increase in the frequencies of the lowest wind speed class (0-10 km h^{-1}) and a decrease in the highest ones, especially for the class > 30 km h^{-1}. In the 2011-2040 period the lowest wind speed frequencies mainly increased in Sicily, Sardinia and Corsica. The highest wind speed class frequencies decreased at a different scale for each subarea showing the larger diminution in Northwest and Northeast Italy and the lower decrease in South and Central Italy. Similar changes were observed for the 2041-2070 period, but in this case slightly higher differences were observed; regarding the 0-10 km h^{-1} wind class, the differences between the subareas were not particularly marked.

3.1.2. Changes in fuel moisture

As described in the Methods section, from the climate projections we derived FFMC and DC codes for the baseline period (1981-2010) and for the two future periods (2011-2040 and 2041-2070), and then we used these codes as indicators of fuel moisture.

The analysis of the baseline data (Annex 2) highlighted that the frequency of ‘moderate’ fuel moisture days for both codes was always greater than 50% but with noticeable differences among the subareas. For both codes, Sicily showed the highest values of ‘dry’, ‘very dry’ and especially ‘extreme’ moisture days (about 10% for dead fuels and 11-12% for live fuels), followed by Sardinia and South Italy. On the contrary, the lowest frequencies of extreme fuel moisture were shown by Northwest and Northeast Italy, being the frequency of ‘moderate’ days more than 95% for both codes. Corsica and Central Italy showed similar fuel moisture frequencies, particularly for fine fuels.

Regarding the variation between the baseline period (1981-2010) and the two future periods (2011-2040 and 2041-2070), in the entire study area the frequency of ‘moderate’ fuel moisture days is expected to decrease for both codes in the two future periods (Fig. 4, Annex 2). The frequencies of the driest categories for FFMC in the 2011-2040 period did not change in Central and Northern areas, while in Sicily, Sardinia and to a lower extent in South Italy, the frequencies of ‘dry’ and ‘very dry’ fuel moisture days slightly increased. However, in the second period (2041-2070), the frequencies of the driest moisture categories increased, except for Northeast and Northwest Italy. The highest increase in the driest categories of FFMC was shown by Sicily followed by Corsica and Central Italy in this second future period.

The changes in DC categories frequencies were in general higher than those in FFMC (Fig. 4, Annex 2). In the 2011-2040 period, the frequency of the days with the highest DC values increased in Corsica and Sardinia and, to a much lower extent, the frequency of ‘very dry’ days in Sicily; the frequency of ‘extreme’ days in Sicily decreased slightly as well as the

frequencies of the driest categories in South Italy. The frequencies of the other subareas did not change in this period. In the 2041-2070 period the changes in DC are more evident. The frequencies of the driest categories increased for all subareas except for Northwest and Northeast Italy, where only the 'very dry' live fuel moisture frequency increased. In this case, Corsica showed the highest increase followed by Central Italy, Sicily and Sardinia.

3.2. Changes in wildfire exposure

From the outputs of RANDIG simulations, a set of fire exposure indicator maps (BP, CFL, FS, Figs. 5-7) was derived for the different study periods and subareas. The highest values of BP, CFL and FS were observed in Sardinia, Corsica and Sicily, while the lowest values were observed in northern areas and Central Italy (Figs. 5-7 and 10, Table IV). Overall, BP and FS changed in a similar way in both future periods and for all subareas (mostly decreasing in the 2011-2040 period and increasing in the 2041-2070 period), whereas the CFL barely varied among periods and subareas (Table IV, Fig. 10).

In particular, in the 2011-2040 period the values of BP and FS with respect to the baseline decreased to a slightly higher extent in Sicily, Central and Northwest Italy, whereas in Sardinia and South Italy the variation was minor. CFL values decreased slightly in this first future period in all subareas. In the 2041-2070 period, Sicily showed the highest increase for BP and FS followed by Central Italy and South Italy; to a much lower extent, BP and FS increased also in Sardinia. On the contrary, BP and average FS decreased in Northwest Italy and Northeast Italy and slightly also in Corsica. The CFL increased slightly in Corsica in this second future period whereas in Northwest Italy, Northeast Italy and Sardinia decreased.

As presented in the Material and Methods section, from the primary fire exposure indicators we derived an extended set of indicators (FPI, HFLP, HFLBP) with the aim to summarize the information on fire probability and severity for the entire study area (Figs. 8 and 9). The evolution of FPI throughout the three studied periods is similar to the evolution of BP or FS (Fig. 10). Regarding the HFLP and HFLBP indicators, results showed limited differences between the three studied periods (Fig. 9, Table IV), except for NE in case of HFLBP and NW in both cases where differences are higher in proportion to their values. The highest mean values of FPI, HFLP, HFLBP were observed in Corsica and Sardinia (Table IV).

In the 2011-2040 period, FPI decreased in all subareas: in Northwest Italy and Sicily the reduction is higher; in Sardinia the decrease is minor; and in the other subareas it ranges from -1.78 to -1.23%. The changes of this index in the 2041-2070 period are different for each subarea. In this period the value of FPI increases for Sicily, Central Italy, South Italy and Sardinia and decreases for Northwest Italy, Northeast Italy and Corsica.

Results provided by ANOVA on all fire exposure indicators (BP, CFL, FS, FPI, HFLP and HFLBP) have shown that the temporal variations between baseline and future periods were significant for $p = 0.01$ in all subareas. Regarding the variations among subareas, the results provided by the post-hoc Student-Newman-Keuls test showed (Table IV) significant differences ($p = 0.01$) for all exposure indices except for NW and NE, where FSs predicted for the two future time periods are similar; some significant similarities were observed between NW and CI, regarding HFLP and FPI; likewise, significant similarities were observed between NW and NE, affecting the HFLP.

4. DICUSSION AND CONCLUSIONS

In this work, we extend our understanding of the potential impact of future climate change on wildfire exposure specifically for the Mediterranean region using a wildfire spread modeling approach. We incorporated projected climate change into a mechanistic wildfire spread modelling system to better represent the effects of fine scale drivers of wildfire propagation on the assessment of climate change impacts. This work is one of the first applications in Europe of a methodology to assess the impacts of climate change on wildfire exposure through a wildfire modeling approach, using both fine resolutions (250 m) and a large assessment scale. Although we used a single climate model rather than an ensemble, the present work contributes methods that can be applied in other areas to analyze different time frames, scenarios, and climate models. The climate projections we used in this study are overall in line with previous works and highlighted an increase in future temperatures and a reduction in precipitation and relative humidity for the entire study area.[22–24] This result is also compatible with the conclusions of the fifth IPCC report that forecasted strong warming trends and precipitation decrease in Southern Europe, with marked increase in number of warm days, heat waves and droughts.[21] We also observed a decrease in average wind speed values and in the frequency of days with strong winds in the future periods for the entire study areas. Although according to the fifth IPCC report[21] there are uncertainties regarding the projections of future wind speed trends, especially during Summer season.[82] However, there is agreement in the decrease of average annual mean wind speed in the study area.[82]

The analysis of the FWI codes (FFMC and DC) highlighted that the frequencies of the 'extreme' fuel moisture categories strongly vary among subareas. In particular, there is a

gradient of the ‘extreme’ fuel moisture frequency from South to North, being the southern subareas characterized by the highest values. The most relevant variations in FFMC and DC were observed in the 2041-2070 period, and the increase in the frequency of the driest days suggests that the fire seasons will be longer than the baseline. A similar finding for Italy was reported by Bedia *et al*.[83,84], who analyzed the future trends in FWI using a multi-model approach considering the SRES-A1B scenario, and observed also a more marked FWI increase in the 2041-2070 period than in the 2011-2040. The lengthening in future fire seasons related to the increased frequency of drier days was also highlighted by other studies.[16,27–29,49,83]

To assess the potential impacts of climate change on wildfire exposure, and to remove possible uncertainties related to future land use changes and therefore variation in fuel types and characteristics (e.g., load, depth, etc), the fuel layer was held constant input for the wildfire simulations of the three periods. For the same reason, we also assumed constant fire ignitions number and location, and we used the historic ignition grids of the period 1990-2008 as a reference for the three study periods.

We observed slight changes in CFL for all periods and for all subareas, primarily because fire intensity is strongly dependent on fuel type, which was held constant. However, climate variations did influence other fire exposure indicators. We found a slight decrease of most of the fire exposure indicators for the first future period and for the entire study area. This was probably related to the decrease in frequency of higher wind speeds. By contrast, in the second future period the values of the fire exposure indicators noticeably increased, probably due to the increase in the frequency of FFMC and DC values associated with extreme

conditions. The different trend in the two periods suggests that probably the fuel moisture content is the most important factor for the fire spread in the study area since a decrease in wind speed in the first future period was able to reduce the exposure indices when the dry fuel conditions increase slightly, whereas a decrease of wind speed from the first to second future periods was not able to counteract the increase of extremely dry fuel conditions. However, there was a high variability among responses in subareas, and for instance the slight increase in the exposure indices in Sardinia in the second future period (2041-2070) and the decreasing trend in Corsica, Northwest Italy and Northeast Italy, confirm that in these regions wind does play a key role. Similar results were provided by Arca *et al.*[49] who studied the fire danger variations in Sardinia using the MTT algorithm and climate data provided by the regional climate model EBU-POM for the IPPC A1B emission scenario. This study showed for the 2071-2100 period an increase in the burn probability associated with an overall increase of the frequency of potential days with extreme fires as measured by the number of days with high values of FWI. Likewise, Kalabokidis *et al.*[51] combined simulations with climate projections from the SRES A1B scenario, in this case derived from simulations of the KNMI regional climate model RACMO2 in Messinia (Greece). They also observed an increase in burn probability at the end of the 21st century.

The differences among subareas are significant for most of the fire exposure indicators. In fact, southern areas and islands showed the highest values for fire exposure variables while northern areas showed the lowest in both present and future periods. These differences were notable even if we used a fixed burn period for all subareas and the number of ignitions was proportional to the size of the study area. Therefore, differences in the fire exposure

indicators among subareas are exclusively due to differences in fuel types, fuel moisture and wind, which are strongly determined by climate conditions.

In conclusion, fire modeling outputs projected an increase in wildfire incidence due to climate change that may lead to several threats in the future. For instance, an increase in greenhouse gas emissions is expected, which in turn favors climate warming.[85–87] Moreover, increasing wildfires might cause substantial changes in the existing vegetation composition and distribution or even desertification of some areas and probably a subsequent erosion.[88–90] Many Mediterranean plants are adapted to cope with fire, but some Mediterranean ecosystems may be strongly affected by wildfires.[86] However, damages in highly valued resources and assets, and human casualties are the most relevant concern.

The main strategy to prevent or minimize future wildfire damages in the Mediterranean basin will be the fuel load reduction and forest management by traditional silvicultural techniques or by alternative solutions.[87,91–95] This approach requires the identification of major concern areas to prioritize interventions. For this purpose, the outputs from our work can be used as a baseline to support the decision making process, aiming at fire management planning and risk mitigation activities. Furthermore, the outputs we obtained can be useful to prioritize specific areas of interest taking into account the affected values, the potential fire behavior or the burn probability, or the landscape physical constraints. This may be done combining GIS analysis and fire exposure maps as key information to plan and evaluate the fuel and fire management activities. Innovative tools, modules and software developed in recent years might also be coupled to fire exposure maps in supporting fire and land managers.[96,72] Further research is now needed to assess how future changes in land cover and ignition patterns will also

contribute to increased fire exposure and risk, and how risk governance systems will adapt to the projected future fire regimes.

FIGURES AND TABLES

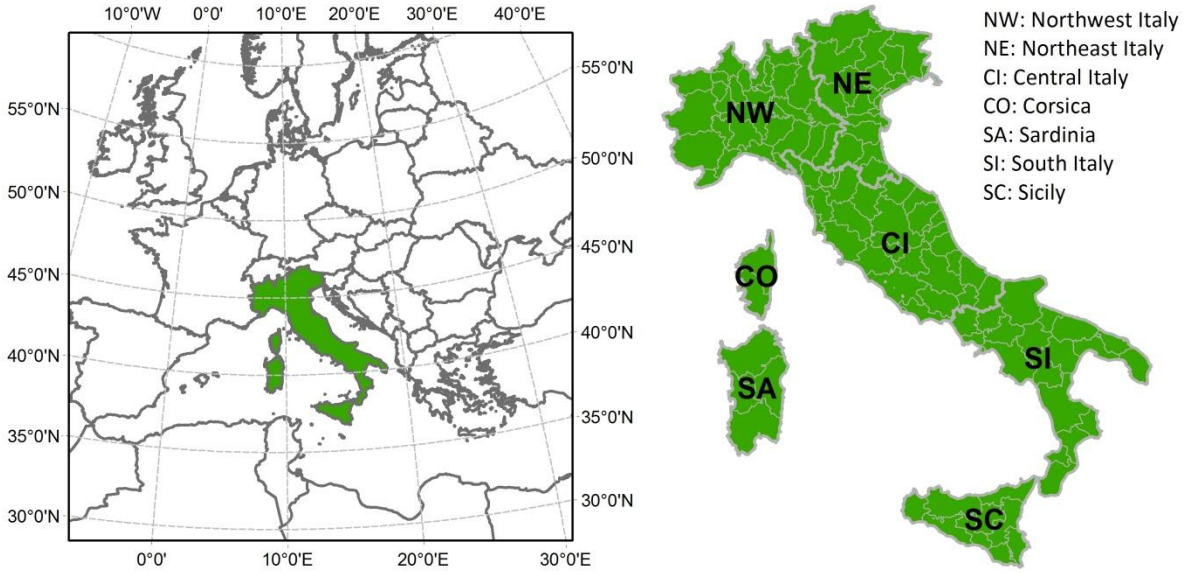

Fig. 1. Location of the study area in the Euro-Mediterranean context (left), and of the seven subareas used in the present study (right).

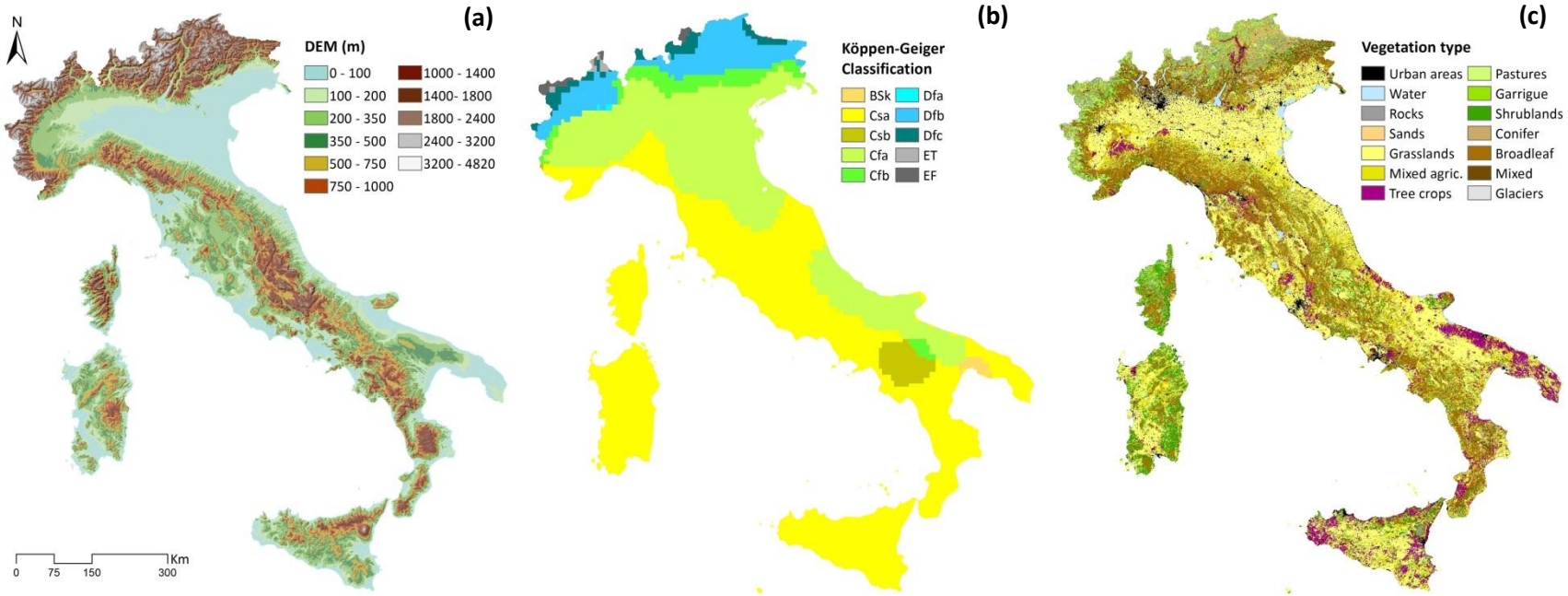

Fig. 2. Digital Elevation Model (a), Koeppen-Geiger climate classification (b), and main vegetation types derived from the Corine land cover map of 2006 (c) of the study area.

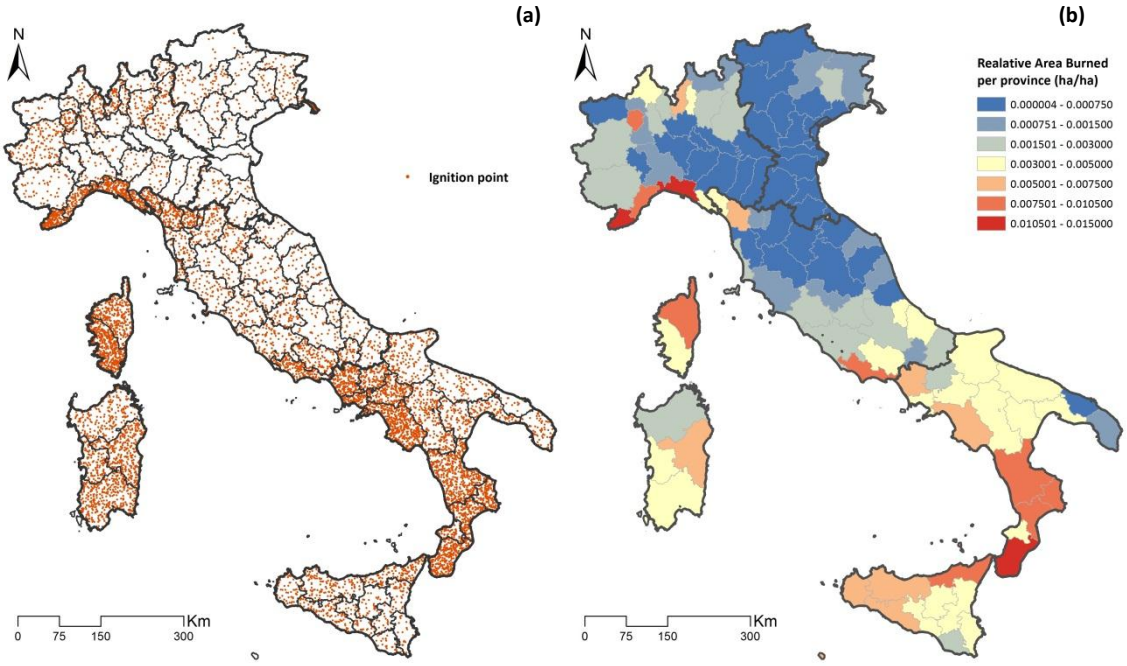

Fig. 3. Average annual fire ignitions at province level (a) and annual area burned relative to the area covered by each province (ha/ha) (b) from historical data (fires occurred from 1990 to 2008, source: JRC).

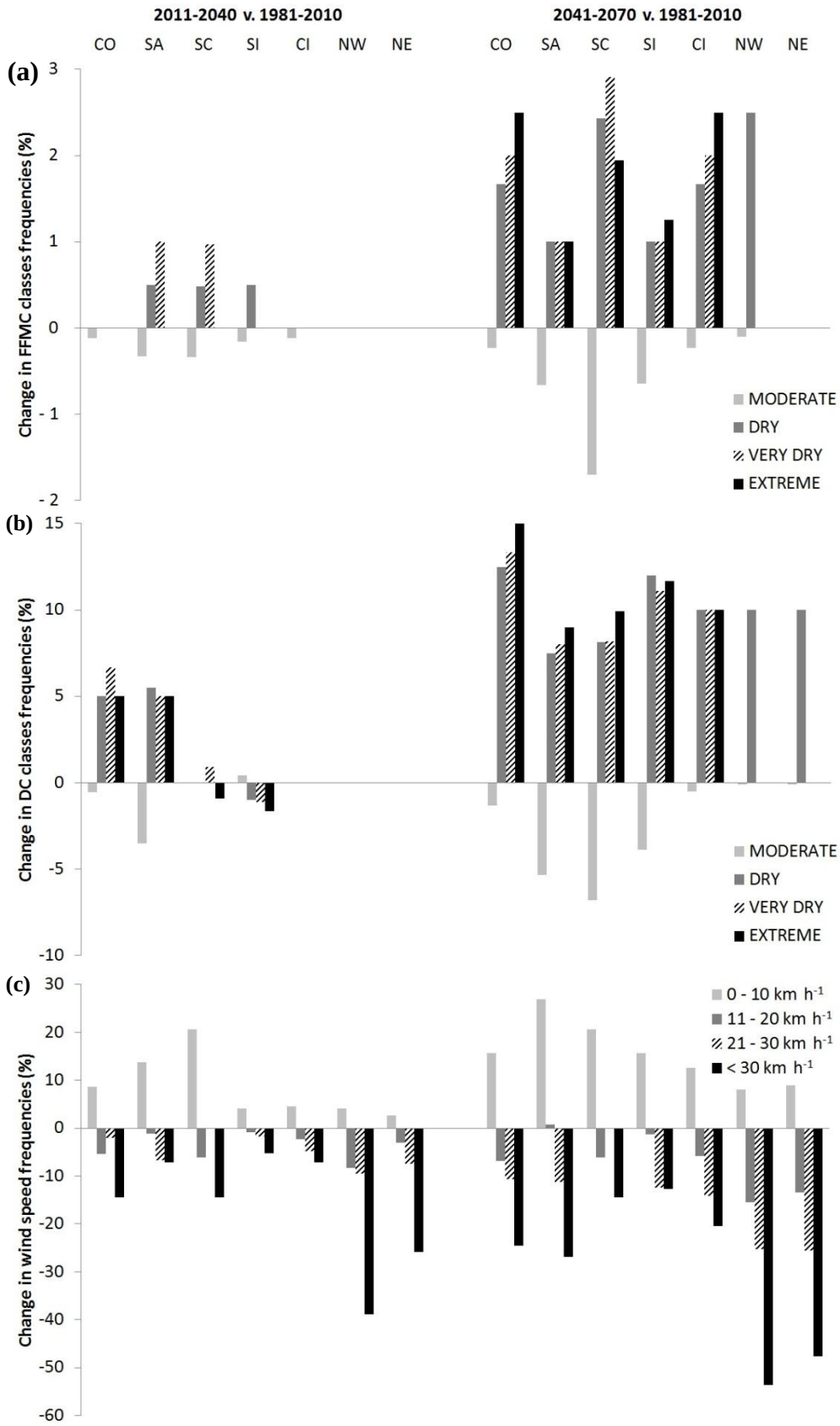
2011-2040 v. 1981-2010
2041-2070 v. 1981-2010
CO SA SC SI CI NW NE
CO SA SC SI CI NW NE
(a)
Change in FFMC classes frequencies (%)
MODERATE
DRY
VERY DRY
EXTREME
(b)
Change in DC classes frequencies (%)
MODERATE
DRY
VERY DRY
EXTREME
(c)
Change in wind speed frequencies (%)
0 - 10 km h-1
11 - 20 km h-1
21 - 30 km h-1
< 30 km h-1

Fig. 4. Variation in FFMC (a), DC (b) and wind speed frequencies (c) from the baseline (1981-2010) to the second (2011-2040) and third (2041-2070) study periods.

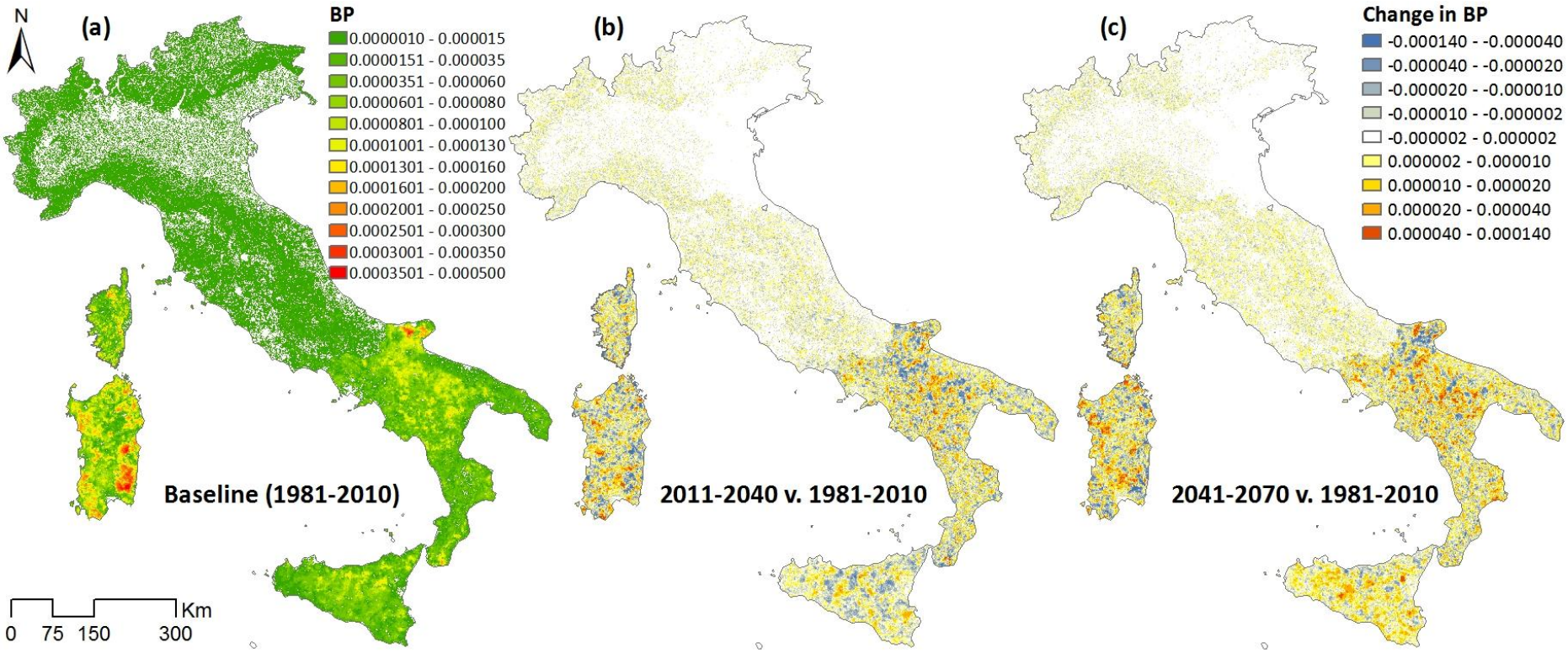

Fig. 5. Maps of Burn Probability (BP): for the baseline period (1981-2010) (a); difference between first future period (2011-2040) and baseline (b); and difference between second future period (2041-2070) and baseline.

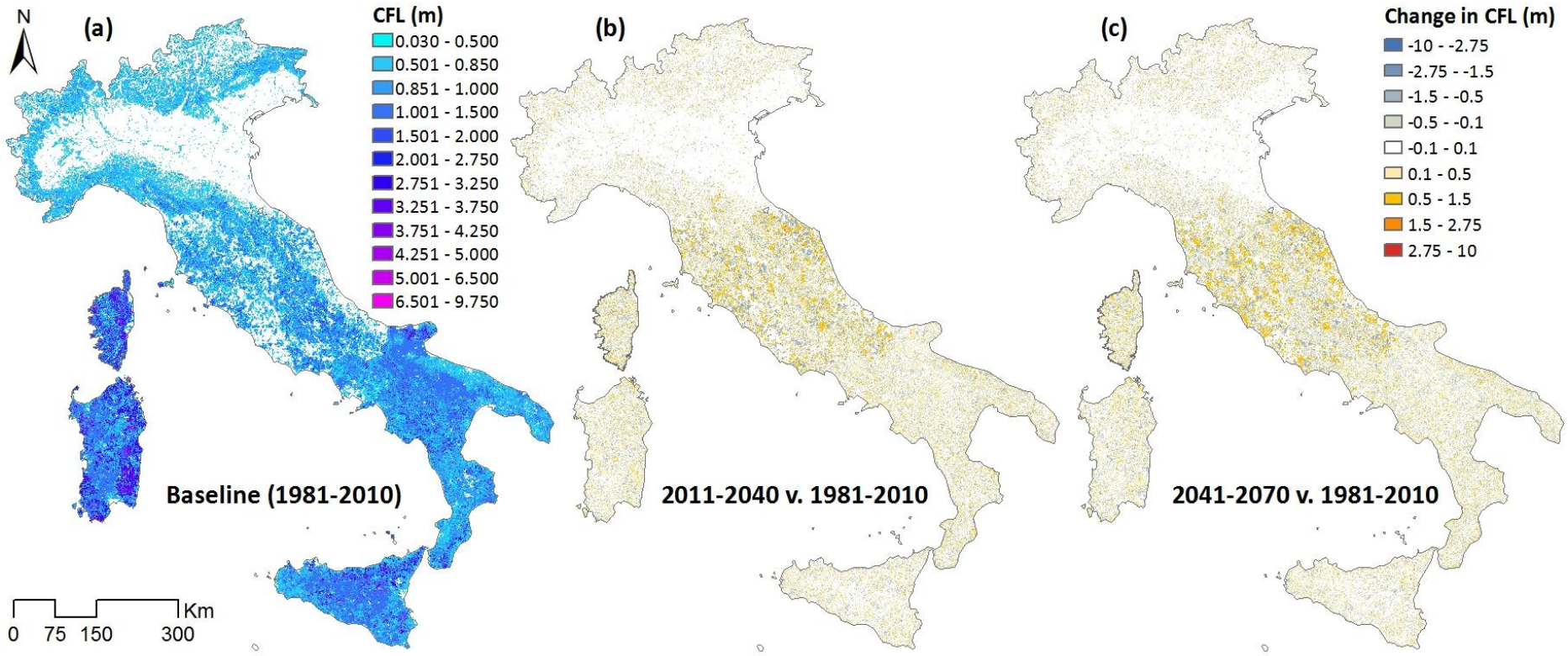

Fig. 6. Maps of Conditional Flame Length (CFL): for the baseline period (1981-2010) (a); difference between first future period (2011-2040) and baseline (b); and difference between second future period (2041-2070) and baseline.

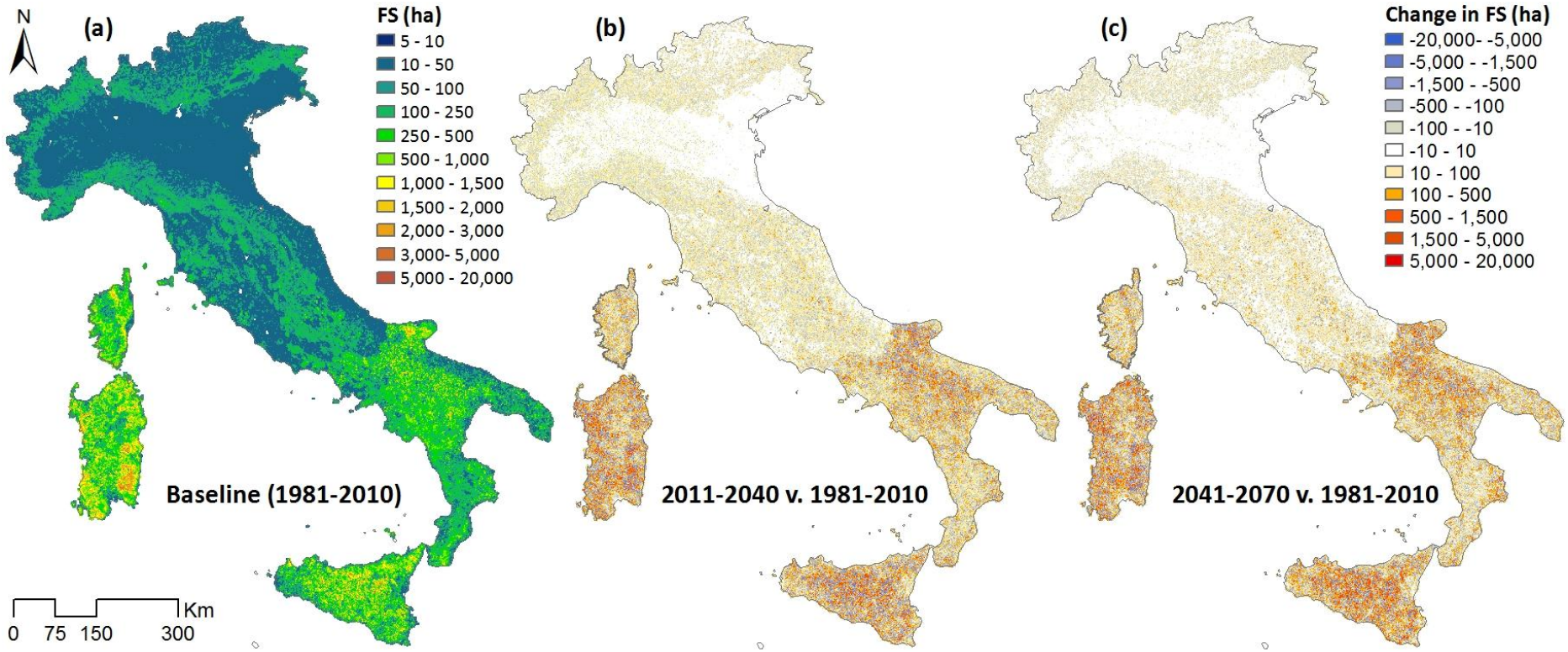

Fig. 7. Maps of Fire Size (FS): for the baseline period (1981-2010) (a); difference between first future period (2011-2040) and baseline (b); and difference between second future period (2041-2070) and baseline.

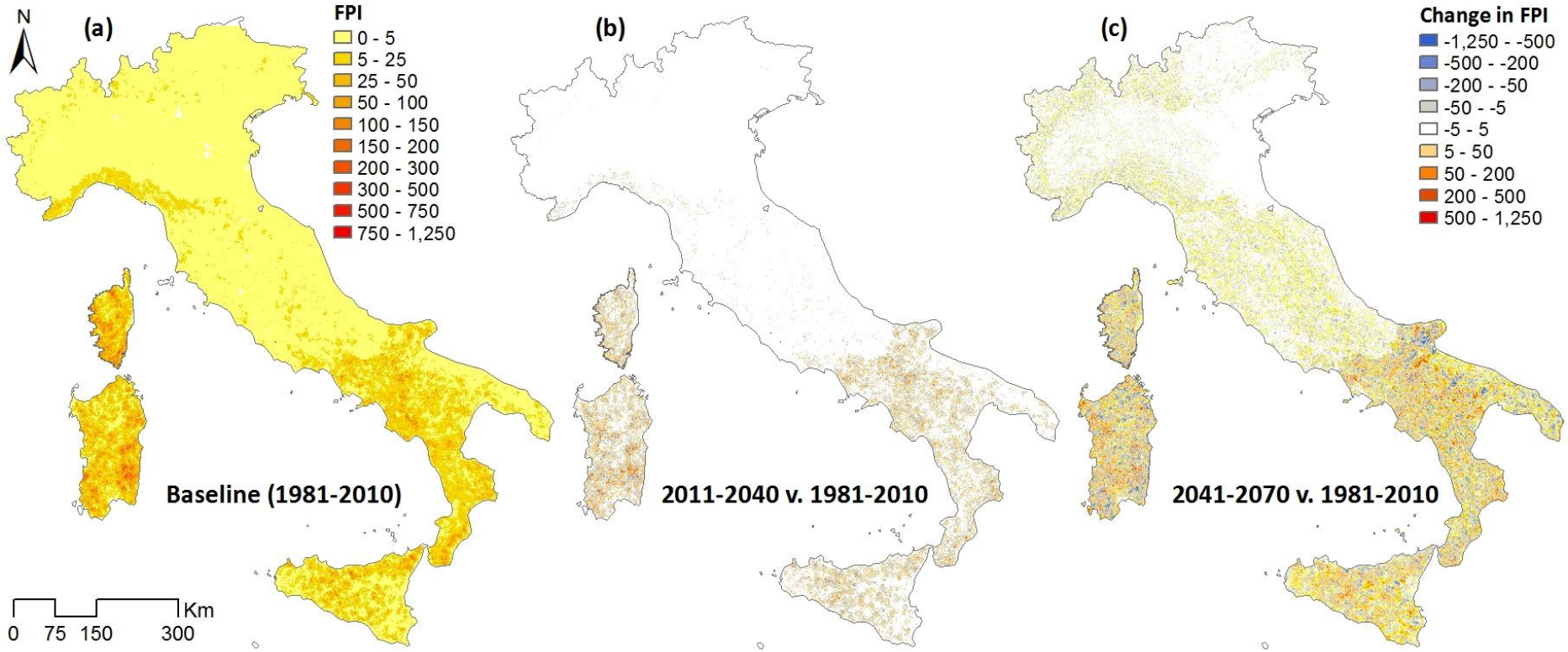

Fig. 8. Maps of Fire Potential Index (FPI) calculated as the product of Fire Size and historical Ignition Probability: for the baseline period (1981-2010) (a); difference between first future period (2011-2040) and baseline (b); and difference between second future period (2041-2070) and baseline.

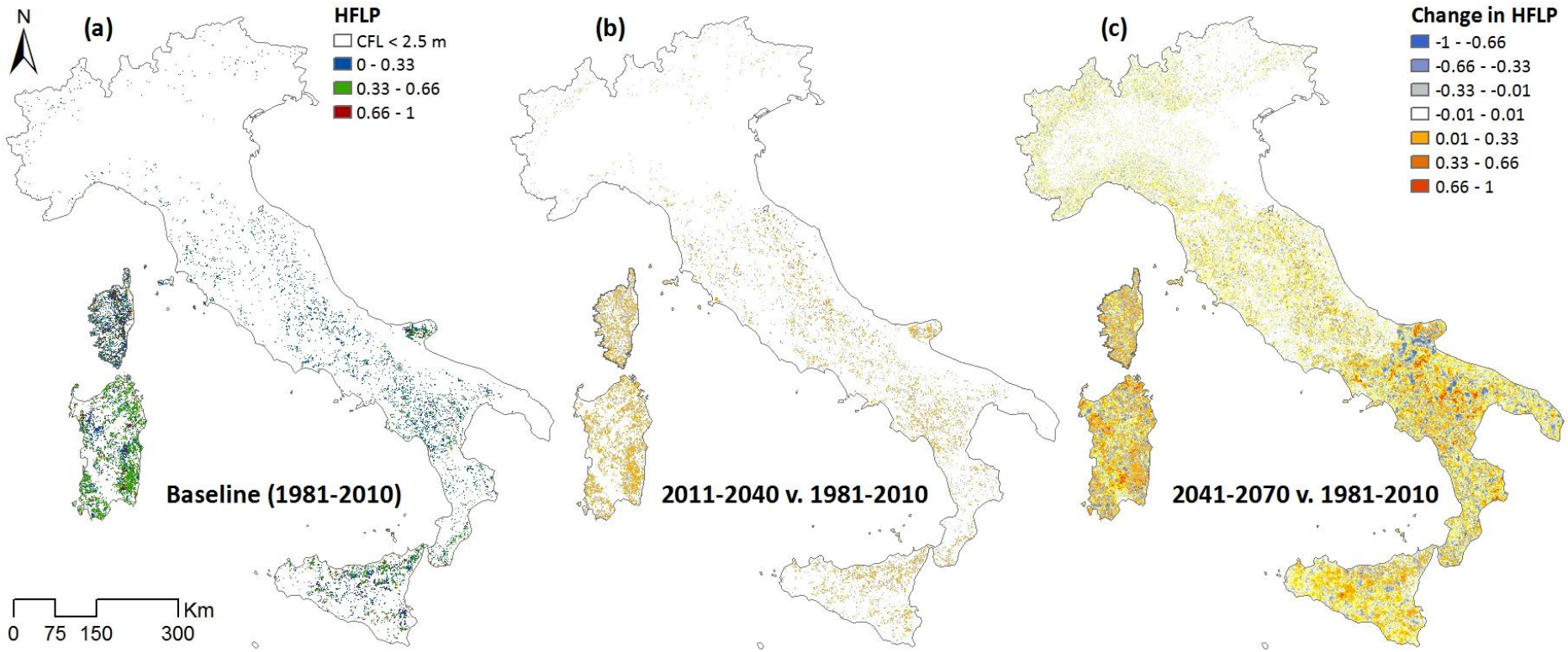

Fig. 9. Maps of High Flame Length Probability (HFLP), which is the probability of high flame length (> 2.5 m) given a fire burning the cell: for the baseline period (1981-2010) (a); difference between first future period (2011-2040) and baseline (b); and difference between second future period (2041-2070) and baseline.

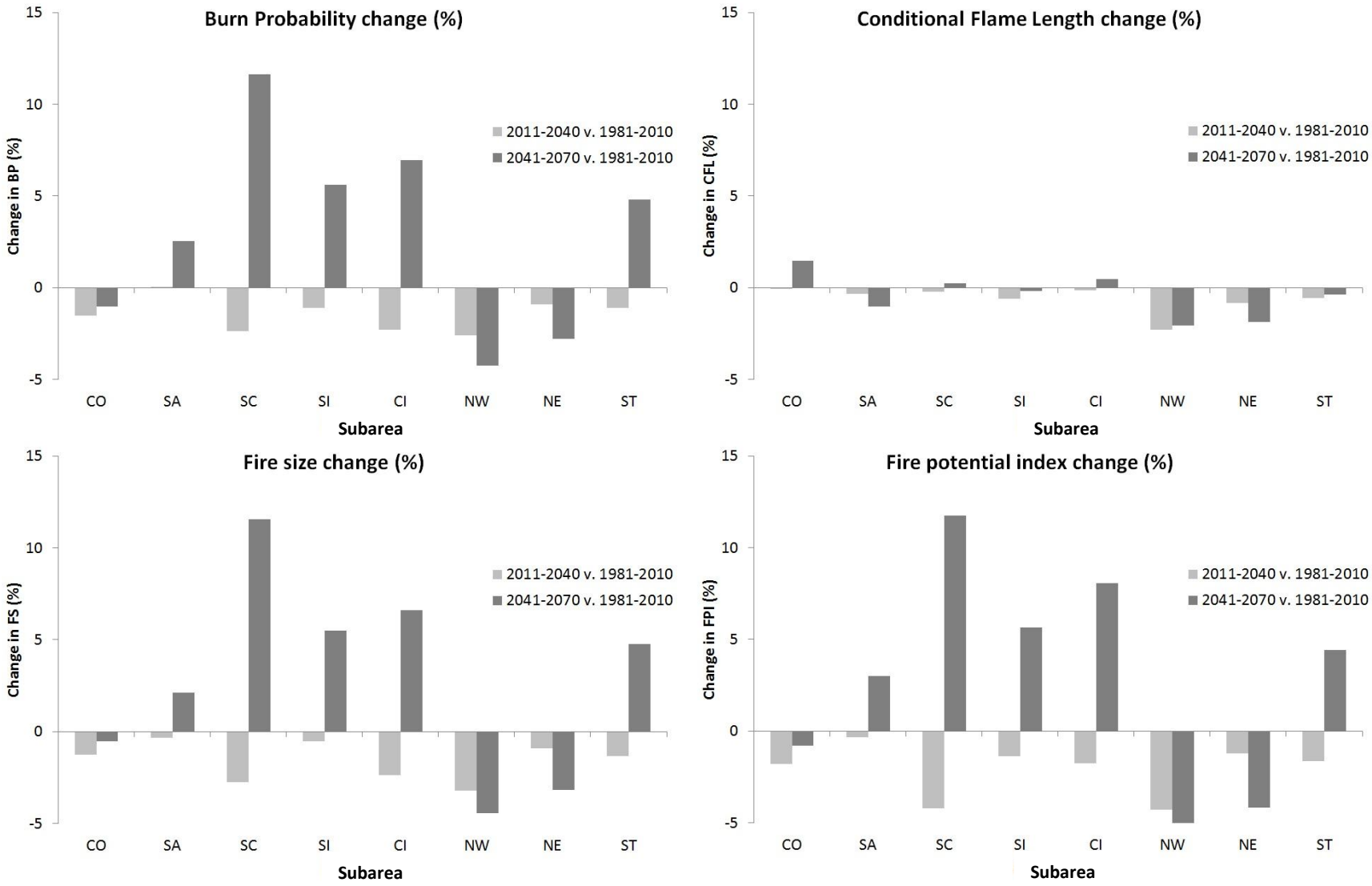
Burn Probability change (%)
Change in BP (%)
2011-2040 v. 1981-2010
2041-2070 v. 1981-2010
Subarea
Conditional Flame Length change (%)
Change in CFL (%)
Fire size change (%)
Change in FS (%)
Fire potential index change (%)
Change in FPI (%)
15
10
5
0
-5
CO
SA
SC
SI
CI
NW
NE
ST

497

Fig. 10. Variation in Burn Probability (BP), Conditional Flame Length (CFL), Fire Size (FS) and Fire Potential Index (FPI) from the baseline (1981-2010) to the second (2011-2040) and third (2041-2070) study periods respectively. The differences were calculated from the outputs of the fire simulations for each subarea and the entire studied area (ST) as follows:

$$Change(\%) = \frac{Value_{future_peiod} - Value_{baseline}}{Value_{baseline}} * 100$$

Table I. Main fuel types and relative incidence. The fuel types were derived from the 2006 Corine Land Cover (CLC) map. To each fuel type, a specific standard or custom fuel model was associated.[45]

Fuel types	**CLC codes**	**Reference Fuel Models used**	**Area (km^2)**	**Incidence (%)**
Urban and anthropic area	1	NB1[56]	14,861	4.80
Water	4; 5	NB8[56]	4,007	1.29
Rocks	332	Mod 1 (reduced load 50%)[55]	4,722	1.53
Sands	331	Mod 1[55]	758	0.24
Grasslands	211; 212; 213; 231	Mod 1[55]	88,579	28.62
Mixed agricultural	241; 242; 243; 244	Mod 1[55]	48,211	15.58
Vineyard and orchard	221; 222; 223	Mod 2[55]	21,610	6.98
Pastures	321	CM 27[57]	15,521	5.02
Garrigue	333; 334	CM 29[57]	4,840	1.56
Mediterranean maquis	322; 323; 324	CM 28[57]	24,880	8.04
Conifer forests	312	TL6[56]	13,259	4.28
Broadleaf forests	311	TL3[56]	56,693	18.32
Mixed forests	313	TU1[56]	11,107	3.59
Glaciers	335	NB8[56]	405	0.13

Table II. Geographic data of the seven subareas identified. The data include administrative region, total area and inhabitants (year of reference 2013),[97,98] and wildfire history from 1990 to 2008.[99]

	Code	Regions included	Total area (km^2)	Inhabitants (million)	Average annual number of fires	Average annual area burned (ha)	Average annual area burned/Total area (%)
Corsica	CO	Corsica	8,716	0.32	302	6,053	0.69
Sardinia	SA	Sardegna	23,909	1.66	1,019	9,898	0.41
Sicily	SC	Sicilia	25,552	5.09	639	14,990	0.64
South Italy	SI	Basilicata, Calabria, Campania, Puglia	58,435	12.52	3,154	32,043	0.55
Central Italy	CI	Abruzzo, Lazio, Marche, Molise, Toscana, Umbria	73,395	13.72	1,628	14,561	0.20
Northwest Italy	NW	Emilia-Romagna (West part), Liguria, Lombardia, Piemonte, Valle d'Aosta	68,926	18.10	1,434	15,203	0.26
Northeast Italy	NE	Emilia-Romagna (East part), Friuli-Venezia, Giulia, Trentino-Alto Adige, Veneto	50,992	9.69	420	2,479	0.05
Entire study area	ST		309,925	61.10	8,597	95,226	0.30

Table III. Ranges of dead and live fuel moisture values (in % of dry weight) used as simulation input data for the different vegetation types. The data where derived from the analysis of different FFMC and DC percentile thresholds (75, 90, 95, 97), using Sardinia as reference.

Moisture category label		**MODERATE**	**DRY**	**VERY DRY**	**EXTREME**
Percentile threshold		$75^{th} – 90^{th}$	$90^{th} – 95^{th}$	$95^{th} – 97^{th}$	$> 97^{th}$
DEAD FUEL	**1 h**	11 - 14	9 - 11	7 - 9	5 - 7
	10h	13 - 16	11 - 13	9 - 11	7 - 9
	100h	15 - 18	13 - 15	11 - 13	9 - 11
LIVE FUEL	**SHRUBS**	110 - 90	90 - 80	80 - 75	75 - 65
	FORESTS	130 - 105	105 - 100	100 - 95	95 - 85

Table IV. Mean values of the different fire exposure indicators calculated for each subarea, for the entire study area (ST), and for each study period (1st timeframe 1981-2010; 2nd timeframe 2011-2040, 3rd timeframe 2041-2070). Values followed by the same letter along the row mean that subareas are not significantly different from each other according to the Student-Newman-Keuls test (for $p = 0.01$); all differences between the baseline and the future time steps are significantly different according to the Student-Newman-Keuls test ($p = 0.01$).

		CO	SA	SC	SI	CI	NW	NE	ST
BP	**1st**	$5.1720\cdot10^{-5}$ **a**	$9.0739\cdot10^{-5}$ **b**	$3.9580\cdot10^{-5}$ **c**	$4.4730\cdot10^{-5}$ **d**	$5.0956\cdot10^{-6}$ **e**	$3.0600\cdot10^{-6}$ **f**	$1.0800\cdot10^{-6}$ **g**	$2.2243\cdot10^{-5}$
	2nd	$5.0930\cdot10^{-5}$ **a**	$9.0740\cdot10^{-5}$ **b**	$3.8640\cdot10^{-5}$ **c**	$4.4240\cdot10^{-5}$ **d**	$4.9781\cdot10^{-6}$ **e**	$2.9800\cdot10^{-6}$ **f**	$1.0700\cdot10^{-6}$ **g**	$2.2001\cdot10^{-5}$
	3rd	$5.1200\cdot10^{-5}$ **a**	$9.3057\cdot10^{-5}$ **b**	$4.4190\cdot10^{-5}$ **c**	$4.7240\cdot10^{-5}$ **d**	$5.4492\cdot10^{-6}$ **e**	$2.9300\cdot10^{-6}$ **f**	$1.0500\cdot10^{-6}$ **g**	$2.3312\cdot10^{-5}$
CFL	**1st**	1.7158 **a**	1.5493 **b**	1.1304 **c**	0.9499 **d**	0.6164 **e**	0.3102 **f**	0.2527 **g**	0.6973
	2nd	1.7150 **a**	1.5440 **b**	1.1279 **c**	0.9444 **d**	0.6157 **e**	0.3031 **f**	0.2506 **g**	0.6934
	3rd	1.7413 **a**	1.5334 **b**	1.1332 **c**	0.9482 **d**	0.6195 **e**	0.3038 **f**	0.2480 **g**	0.6948
FS	**1st**	444.7256 **a**	743.3677 **b**	540.4703 **c**	284.2069 **d**	78.8086 **e**	50.5048 **f**	43.2407 **g**	205.2689
	2nd	439.1410 **a**	740.7777 **b**	525.6507 **c**	282.6651 **d**	76.9429 **e**	48.8820 **f**	42.8441 **f**	202.5211
	3rd	442.3663 **a**	759.1505 **b**	603.0428 **c**	299.8642 **d**	84.0047 **e**	48.2669 **f**	41.8648 **f**	215.0340
FPI	**1st**	38.4007 **a**	30.9625 **b**	13.0511 **c**	13.8969 **d**	1.7928 **e**	1.4609 **e**	0.4047 **f**	7.9804
	2nd	37.7167 **a**	30.8614 **b**	12.5008 **c**	13.7108 **d**	1.7644 **e**	1.3962 **e**	0.4006 **f**	7.8509
	3rd	38.0890 **a**	31.8974 **b**	14.5849 **c**	14.6820 **c**	1.9384 **d**	1.3800 **e**	0.3885 **f**	8.3325
HFLP	**1st**	$2.0180\cdot10^{-1}$ **a**	$1.5031\cdot10^{-1}$ **b**	$5.7811\cdot10^{-2}$ **c**	$2.8831\cdot10^{-2}$ **d**	$9.5917\cdot10^{-3}$ **e**	$7.3840\cdot10^{-4}$ **f**	$6.2250\cdot10^{-4}$ **f**	$2.9893\cdot10^{-2}$
	2nd	$2.0305\cdot10^{-1}$ **a**	$1.5128\cdot10^{-1}$ **b**	$5.7589\cdot10^{-2}$ **c**	$2.8489\cdot10^{-2}$ **d**	$9.6256\cdot10^{-3}$ **e**	$3.5930\cdot10^{-4}$ **f**	$6.2960\cdot10^{-4}$ **f**	$3.0493\cdot10^{-2}$
	3rd	$2.0536\cdot10^{-1}$ **a**	$1.4992\cdot10^{-1}$ **b**	$5.9475\cdot10^{-2}$ **c**	$2.9232\cdot10^{-2}$ **d**	$9.7861\cdot10^{-3}$ **e**	$5.0400\cdot10^{-4}$ **f**	$6.1130\cdot10^{-4}$ **f**	$3.0632\cdot10^{-2}$
HFLBP	**1st**	$3.7389\cdot10^{-4}$ **a**	$1.9050\cdot10^{-4}$ **b**	$5.4760\cdot10^{-5}$ **c**	$7.0500\cdot10^{-6}$ **d**	$4.9239\cdot10^{-7}$ **e**	$4.0000\cdot10^{-8}$ **e**	$4.0000\cdot10^{-8}$ **e**	$3.1049\cdot10^{-5}$
	2nd	$3.6356\cdot10^{-4}$ **a**	$1.8900\cdot10^{-4}$ **b**	$5.3070\cdot10^{-5}$ **c**	$6.9600\cdot10^{-6}$ **d**	$4.8936\cdot10^{-7}$ **e**	$2.0000\cdot10^{-8}$ **e**	$5.0000\cdot10^{-8}$ **e**	$3.2161\cdot10^{-5}$
	3rd	$3.6356\cdot10^{-4}$ **a**	$1.8900\cdot10^{-4}$ **b**	$5.3070\cdot10^{-5}$ **c**	$6.9600\cdot10^{-6}$ **d**	$4.8936\cdot10^{-7}$ **e**	$2.0000\cdot10^{-8}$ **e**	$5.0000\cdot10^{-8}$ **e**	$3.2164\cdot10^{-5}$

REFERENCES

1. Cole DN, Landres PB. Threats to wilderness ecosystems: impacts and research needs. Ecological Applications, 1996; 6(1):168–184.
2. Syphard AD, Radeloff VC, Hawbaker TJ, Stewart SI. Conservation Threats Due to Human-Caused Increases in Fire Frequency in Mediterranean-Climate Ecosystems. Conservation Biology, 2009; 23(3):758–769.
3. Haas JR, Calkin DE, Thompson MP. Wildfire Risk Transmission in the Colorado Front Range, USA. Risk Analysis, 2015; 35(2):226–240.
4. FAO. State of Mediterranean Forests 2013. Food and Agriculture Organization of the United Nations; 2013. 191 p
5. Martínez J, Vega-Garcia C, Chuvieco E. Human-caused wildfire risk rating for prevention planning in Spain. Journal of Environmental Management, 2009; 90(2):1241–1252.
6. Pausas JG, Keeley JE. A Burning Story: The Role of Fire in the History of Life. BioScience, 2009; 59(7):593–601.
7. Baeza MJ, De Luís M, Raventós J, Escarré A. Factors influencing fire behaviour in shrublands of different stand ages and the implications for using prescribed burning to reduce wildfire risk. Journal of Environmental Management, 2002; 65(2):199–208.
8. Cary GJ, Flannigan MD, Keane RE, Bradstock RA, Davies ID, Lenihan JM, Li C, Logan KA, Parsons RA. Relative importance of fuel management, ignition management and weather for area burned: evidence from five landscape–fire–succession models. International Journal of Wildland Fire, 2009; 18(2):147.
9. Dube OP. Linking fire and climate: interactions with land use, vegetation, and soil. Current Opinion in Environmental Sustainability, 2009; 1(2):161–169.
10. Pechony O, Shindell DT. Driving forces of global wildfires over the past millennium and the forthcoming century. In Proceedings of the National Academy of Sciences. Vol 107. 2010, p. 19167–19170.
11. Ager AA, Preisler HK, Arca B, Spano D, Salis M. Wildfire risk estimation in the Mediterranean area. Environmetrics, 2014; 25(6):384–396.
12. Flannigan MD, Stocks BJ, Wotton BM. Climate change and forest fires. Science of The Total Environment, 2000; 262(3):221–229.
13. Flannigan M, Stocks B, Turetsky M, Wotton M. Impacts of climate change on fire activity and fire management in the circumboreal forest. Global Change Biology, 2009; 15(3):549–560.
14. Liu Y, Goodrick SL, Stanturf JA. Future U.S. wildfire potential trends projected using a dynamically downscaled climate change scenario. Forest Ecology and Management, 2013; 294:120–135.
15. Brown TJ, Hall BL, Westerling AL. The impact of twenty-first century climate change on wildland fire danger in the western united states: An applications perspective. Climatic Change, 2004; 62(1-3):365–388.
16. Moriondo M, Good P, Durao R, Bindi M, Giannakopoulos C, Corte-Real J. Potential impact of climate change on fire risk in the Mediterranean area. Climate Research, 2006; 31:85–95.
17. Mouillot F, Rambal S, Joffre R. Simulating climate change impacts on fire frequency and vegetation dynamics in a Mediterranean-type ecosystem. Global Change Biology, 2002; 8(5):423–437.
18. Turco M, Llasat M-C, von Hardenberg J, Provenzale A. Climate change impacts on wildfires in a Mediterranean environment. Climatic Change, 2014; 125(3-4):369–380.
19. Piñol J, Terradas J, Lloret F. Climate warming, wildfire hazard, and wildfire occurrence in coastal eastern

Spain. Climatic Change, 1998; 38(3):345–357.

20. Westerling AL, Hidalgo HG, Cayan DR, Swetnam TW. Warming and Earlier Spring Increase Western U.S. Forest Wildfire Activity. Science, 2006; 313(5789):940–943.

21. IPCC. Climate Change 2014: Impacts, Adaptation, and Vulnerability. Part B: Regional Aspects. Cambridge, United Kingdom and New York, NY, USA: Intergovernmental Panel on Climate Change, Cambridge University Press; 2014. 1689-1699 p. Report No.: Fifth Assessment Report

22. Beniston M, Stephenson DB, Christensen OB, Ferro CAT, Frei C, Goyette S, Halsnaes K, Holt T, Jylhä K, Koffi B, Palutikof J, Schöll R, Semmler T, Woth K. Future extreme events in European climate: an exploration of regional climate model projections. Climatic Change, 2007; 81(S1):71–95.

23. Kjellström E, Nikulin G, Hansson U, Strandberg G, Ullerstig A. 21st century changes in the European climate: Uncertainties derived from an ensemble of regional climate model simulations. Tellus, Series A: Dynamic Meteorology and Oceanography, 2011; 63(1):24–40.

24. Feyen L, Dankers R. Impact of global warming on streamflow drought in Europe. Journal of Geophysical Research: Atmospheres, 2009; 114(17):1–17.

25. Flannigan MD, Krawchuk MA, de Groot WJ, Wotton BM, Gowman LM. Implications of changing climate for global wildland fire. International Journal of Wildland Fire, 2009; 18(5):483–507.

26. Van Wagner CE. Development and Structure of the Canadian Forest Fire Weather Index System. Ottawa: Canadian Forestry Service, Petawawa National Forestry Institute; 1987. 48 p. Report No.: Forestry Technical Report 35

27. Carvalho AC, Carvalho A, Martins H, Marques C, Rocha A, Borrego C, Viegas DX, Miranda AI. Fire weather risk assessment under climate change using a dynamical downscaling approach. Environmental Modelling & Software, 2011; 26(9):1123–1133.

28. Pellizzaro G, Ventura A, Arca B, Arca A, Duce P, Bacciu V, Spano D. Estimating effects of future climate on duration of fire danger season in Sardinia. In Viegas DX (ed). Proceedings of VI International Forest Fire Research Conference. Coimbra, 2010, p. 8.

29. Karali A, Hatzaki M, Giannakopoulos C, Roussos A, Xanthopoulos G, Tenentes V. Sensitivity and evaluation of current fire risk and future projections due to climate change: the case study of Greece. Natural Hazards and Earth System Science, 2014; 14(1):143–153.

30. Lung T, Lavalle C, Hiederer R, Dosio A, Bouwer LM. A multi-hazard regional level impact assessment for Europe combining indicators of climatic and non-climatic change. Global Environmental Change, 2013; 23(2):522–536.

31. Dury M, Hambuckers A, Warnant P, Henrot A, Favre E, Ouberdous M, Fran Ois L. Responses of European forest ecosystems to 21 st century climate: assessing changes in interannual variability and fire intensity. iForest Biogeosciences and Forestry, 2011; 4(2):82–99.

32. Botequim B, Garcia-Gonzalo J, Marques S, Ricardo a, Borges J, Tomé M, Oliveira M. Developing wildfire risk probability models for Eucalyptus globulus stands in Portugal. iForest - Biogeosciences and Forestry, 2013; 6(4):217–227.

33. Chuvieco E, Aguado I, Yebra M, Nieto H, Salas J, Martín MP, Vilar L, Martínez J, Martín S, Ibarra P, de la Riva J, Baeza J, Rodríguez F, Molina JR, Herrera MA, et al. Development of a framework for fire risk assessment using remote sensing and geographic information system technologies. Ecological Modelling, 2010; 221(1):46–58.

34. Finney MA. The challenge of quantitative risk analysis for wildland fire. Forest Ecology and Management, 2005; 211(1-2):97–108.

35. Chuvieco E, Allgöwer B, Salas J. Integration of Physical and Human Factors in Fire Danger Assessment. In Chuvieco E (ed). Wildland Fire Danger Estimation and Mapping: The Role of Remote Sensing Data. Series in Remote Sensing, Vol. 4. Singapore: World Scientific Publishing, 2003, p. 197–218.

36. Verde JC, Zêzere JL. Assessment and validation of wildfire susceptibility and hazard in Portugal. Natural Hazards and Earth System Science, 2010; 10(3):485–497.

37. Scott JH, Thompson MP, Calkin DE. A Wildfire Risk Assessment Framework for Land and Resource Management. 2013; (October).

38. Ager AA, Buonopane M, Reger A, Finney MA. Wildfire Exposure Analysis on the National Forests in the Pacific Northwest, USA. Risk Analysis, 2013; 33(6):1000–1020.

39. Finney MA, McHugh CW, Grenfell IC, Riley KL, Short KC. A simulation of probabilistic wildfire risk components for the continental United States. Stochastic Environmental Research and Risk Assessment, 2011; 25(7):973–1000.

40. Finney MA. An Overview of FlamMap Fire Modeling Capabilities. In Andrews PL, Butler BW (eds). Fuel Management-How to Measure Success: Conference Proceedings. 28-30 March. Portland, OR: USDA Forest Service, Rocky Mountain Research Station, RMRS-P-41, 2006, p. 213–220.

41. Ager AA, Vaillant NM, Finney MA, Preisler HK. Analyzing wildfire exposure and source–sink relationships on a fire prone forest landscape. Forest Ecology and Management, 2012; 267:271–283.

42. Gomez C, Mangeas M, Curt T, Ibanez T, Munzinger J, Dumas P, Jérémy A, Despinoy M, Hély C. Wildfire Risk for Main Vegetation Units in a Biodiversity Hotspot: Modeling Approach in New Caledonia, South Pacific. Ecology and Evolution, 2015; 5(2):377–390.

43. Haas JR, Calkin DE, Thompson MP. A national approach for integrating wildfire simulation modeling into Wildland Urban Interface risk assessments within the United States. Landscape and Urban Planning, 2013; 119:44–53.

44. Ager AA, Day MA, McHugh CW, Short K, Gilbertson-Day J, Finney MA, Calkin DE. Wildfire exposure and fuel management on western US national forests. Journal of Environmental Management, 2014; 145:54–70.

45. Salis M, Ager AA, Arca B, Finney MA, Bacciu V. Assessing exposure to human and ecological values in Sardinia, Italy. International Journal of Wildland Fire, 2013; 22:549–565.

46. Alcasena FJ, Salis M, Ager A a., Arca B, Molina D, Spano D. Assessing Landscape Scale Wildfire Exposure for Highly Valued Resources in a Mediterranean Area. Environmental Management, 2015:1200–1216.

47. Parisien MA, Walker GR, Little JM, Simpson BN, Wang X, Perrakis DDB. Considerations for modeling burn probability across landscapes with steep environmental gradients: An example from the Columbia Mountains, Canada. Natural Hazards, 2013; 66(2):439–462.

48. Miller C, Ager AA. A review of recent advances in risk analysis for wildfire management. International Journal of Wildland Fire, 2013; 22(1):1–14.

49. Arca B, Pellizzaro G, Duce P, Salis M, Bacciu V, Spano D, Ager AA, Scoccimarro E. Potential changes in fire probability and severity under climate change scenarios in mediterranean areas. In Spano D, Bacciu V, Salis M, Sirca C (eds). International Conference on Fire Behaviour and Risk. Alghero, Sardinia (Italy), 2012, p. 92–98.

50. Mitsopoulos I, Mallinis G, Karali A, Giannakopoulos C, Arianoutsou M. Mapping fire behaviour in a Mediterranean landscape under different future climate change scenarios. In Adapt to Climate. Nicosia, Cyprus, 2014, p. 11.

51. Kalabokidis K, Palaiologou P, Gerasopoulos E, Giannakopoulos C, Kostopoulou E, Zerefos C. Effect of Climate Change Projections on Forest Fire Behavior and Values-at-Risk in Southwestern Greece. Forests,

2015; 6(6):2214–2240.

52. Peel MC, Finlayson BL, McMahon TA. Updated world map of the Köppen-Geiger climate classification. Hydrology and Earth System Sciences, 2007; 11(5):1633–1644.

53. EEA. Version 15 of Raster Data on Land Cover for the Corine Land Cover 2006 Inventory. European Environmental Agency; 2011. Available at: http://www.eea.europa.eu/data-and-maps/data/corine-land-cover-2006-raster-1

54. CGIAR-CSI. Resolution, Version 4 of Srtm Digital Elevation Model of 90m. CGIAR Consortium for Spatial Information; 2008. Available at: http://srtm.csi.cgiar.org

55. Anderson HE. Aids to Determining Fuel Models for Estimating Fire Behavior. Ogden, UT: USDA Forest Service, Intermountain Forest and Range Experiment Station; 1982. 22 p. Report No.: General Technical Report INT-122.

56. Scott JH, Burgan RE. Standard Fire Behavior Fuel Models: A Comprehensive Set for Use with Rothermel's Surface Fire Spread Model. Fort Collins (CO): USDA Forest Service, Rocky Mountain Research Station; 2005. 80 p. Report No.: General Technical Report RMRS-GTR-153

57. Arca B, Bacciu V, Pellizzaro G, Salis M, Ventura A, Duce P, Brundu G. Fuel model mapping by Ikonos imagery to support spatially explicit fire simulators. In 7th International Workshop on Advances in Remote Sensing and GIS Applications in Forest Fire Management towards an Operational Use of Remote Sensing in Forest Fire Management. Matera, 2009, p. 4.

58. INFC. Secondo Inventario Nazionale Delle Foreste E Dei Serbatoi Forestali Di Carbonio. Ministero delle Politiche Agricole Alimentari e Forestali, Ispettorato Generale – Corpo Forestale dello Stato; CRA – Istituto Sperimentale per l'Assestamento Forestale e per l'Alpicoltura; 2005

59. IPCC. Climate Change 2007. Cambridge, United Kingdom and New York, NY, USA: Intergovernmental Panel on Climate Change; 2007. Report No.: Fourth Assessment Report

60. IPCC. Evaluation of Climate Models. Cambridge, United Kingdom and New York, NY, USA: Intergovernmental Panel on Climate Change, Cambridge University Press; 2013. 741-866 p. Report No.: Fifth Assessment Report

61. Rockel B, Will A, Hense A. The Regional Climate Model COSMO-CLM (CCLM). Meteorologische Zeitschrift, 2008; 17(4):347–348.

62. Gualdi S, Somot S, May W, Castellari S, Déqué M, Adani M, Artale V, Bellucci A, Breitgand JS, Carillo A, Cornes R, Dell'Aquila A, Dubois C, Efthymiadis D, Elizalde A, et al. Future Climate Projections. In Navarra A, Tubiana L (eds). Regional Assessment of Climate Change in the Mediterranean.

63. Gualdi S, Somot S, Li L, Artale V, Adani M, Bellucci A, Braun A, Calmanti S, Carillo A, Dell'Aquila A, Déqué M, Dubois C, Elizalde A, Harzallah A, Jacob D, et al. Regional Climate Change Projections with Realistic. Bulletin of the American Meteorological Society, 2013; 94:65–81.

64. Steppeler J, Doms G, Schättler U, Bitzer HW, Gassmann A, Damrath U, Gregoric G. Meso-gamma scale forecasts using the nonhydrostatic model LM. Meteorology and Atmospheric Physics, 2003; 82(1-4):75–96.

65. Groot WJ De, Field RD, Brady MA, Roswintiarti O, Mohamad M. Development of the Indonesian and Malaysian Fire Danger Rating Systems. Mitigation and Adaptation Strategies for Global Change, 2006; 12(1):165–180.

66. Viegas DX, Piñol J, Viegas MT, Ogaya R. Estimating live fine fuels moisture content using meteorologically-based indices. International Journal of Wildland Fire, 2001; 10(2):223–240.

67. Pellizzaro G, Duce P, Ventura A, Zara P. Seasonal variations of live moisture content and ignitability in shrubs of the mediterranean basin. International Journal of Wildland Fire, 2007; 16(5):633–641.

68. Salis M, Ager AA, Alcasena FJ, Arca B, Finney MA, Pellizzaro G, Spano D. Analyzing seasonal patterns of wildfire exposure factors in Sardinia, Italy. Environmental Monitoring and Assessment, 2015; 187(1):4175.

69. Pellizzaro G, Cesaraccio C, Duce P, Ventura A, Zara P. Influence of seasonal weather variations and vegetative cycle on live moisture content and ignitability in Mediterranean maquis species. Forest Ecology and Management, 2006; 234:111.

70. Pellizzaro G, Ventura A, Arca B, Arca A, Duce P. Weather seasonality and temporal pattern of live and dead fuel moisture content in Mediterranean shrubland. Geophysical Research Abstracts, 2009; 11:12100–12100.

71. Finney MA. Fire growth using minimum travel time methods. Canadian Journal of Forest Research, 2002; 32(8):1420–1424.

72. Ager AA, Vaillant NM, Finney MA. Integrating Fire Behavior Models and Geospatial Analysis for Wildland Fire Risk Assessment and Fuel Management Planning. Journal of Combustion, 2011; 2011:1–19.

73. Rothermel RC. A Mathematical Model for Predicting Fire Spread in Wildland Fuels. Ogden, UT: USDA Forest Service, Intermountain Forest and Range Experiment Station; 1972. Report No.: Research paper INT-115

74. Van Wagner CE. Conditions for the start and spread of crown fire. Canadian Journal of Forest Research, 1977; 7:23–34.

75. Scott JH, Reinhardt ED. Assessing Crown Fire Potential by Linking Models of Surface and Crown Fire Behavior. Fort Collins, CO: Usda Forest Service Rocky Mountain Research Station; 2001. 59 p. Report No.: Research paper RMRS-RP-29

76. Forthofer JM, Butler BW, Mchugh CW, Finney MA, Bradshaw LS, Stratton RD, Shannon KS, Wagenbrenner NS. A comparison of three approaches for simulating fine-scale surface winds in support of wildland fire management . Part II . An exploratory study of the effect of simulated winds on fire growth simulations. International Journal of Wildland Fire, 2014; (Finney 1998):1–13.

77. Forthofer JM, Butler BW, Mchugh CW, Finney MA, Bradshaw LS, Stratton RD, Shannon KS, Wagenbrenner NS. A comparison of three approaches for simulating fine-scale surface winds in support of wildland fire management . Part II . An exploratory study of the effect of simulated winds on fire growth simulations. International Journal of Wildland Fire, 2014:1–13.

78. Wilson R. Reformulation of of Forest Fire Spread Equations in SI Units. Ogden, UT: USDA Forest Service, Intermountain Forest and Range Experiment Station; 1980. 5 p. Report No.: Research Note INT-292

79. Byram GM. Combustian of Fuels. In Davis KP (ed). Forest Fire Control and Use. New York, Toronto, London: McGraw-Hill Book Company, 1959, p. 61–89.

80. Christiensen R. Plane Answers to Complex Questions: The Theory of Linear Models. 3rd ed. New York: Springer, 2002.

81. R Core Team. R: A language and environment for statistical computing. 2013.

82. McInnes KL, Erwin T a., Bathols JM. Global Climate Model projected changes in 10 m wind speed and direction due to anthropogenic climate change. Atmospheric Science Letters, 2011; 12(4):325–333.

83. Bedia J, Herrera S, Camia a., Moreno JM, Gutiérrez JM. Forest fire danger projections in the Mediterranean using ENSEMBLES regional climate change scenarios. Climatic Change, 2014; 122(1-2):185–199.

84. Bedia J, Herrera S, Camia A, Moreno JM, Gutiérrez JM. Erratum to: Forest fire danger projections in the Mediterranean using ENSEMBLES regional climate change scenarios. Climatic Change, 2014; 122(1-2):185–199.

85. Chiriacò MV, Perugini L, Cimini D, D'Amato E, Valentini R, Bovio G, Corona P, Barbati A. Comparison of approaches for reporting forest fire-related biomass loss and greenhouse gas emissions in southern

Europe. International Journal of Wildland Fire, 2013; 22:730–738.

86. Pausas JG, Llovet J, Anselm R, Vallejo R. Are wildfires a disaster in the Mediterranean basin ? – A review Vegetation changes Shrublands dominated by resprouting species. International Journal of Wildland Fire, 2008:1–22.

87. Vilén T, Fernandes PM. Forest Fires in Mediterranean Countries: CO(2) Emissions and Mitigation Possibilities Through Prescribed Burning. Environmental management, 2011; 48(3):558–567.

88. Guiomar N, Godinho S, Fernandes PM, Machado R, Neves N, Fernandes JP. Wildfire patterns and landscape changes in Mediterranean oak woodlands. Science of The Total Environment, 2015; 536:338–352.

89. Vacchiano G, Motta R. An improved species distribution model for Scots pine and downy oak under future climate change in the NW Italian Alps. Annals of Forest Science, 2014:1–14.

90. Karamesouti M, Petropoulos GP, Papanikolaou ID, Kairis O, Kosmas K. Erosion rate predictions from PESERA and RUSLE at a Mediterranean site before and after a wildfire: Comparison & implications. Geoderma, 2016; 261:44–58.

91. Marino E, Hernando C, Madrigal J, Guijarro M. Short-term effect of fuel treatments on fire behaviour in a mixed heathland: a comparative assessment in an outdoor wind tunnel. International Journal of Wildland Fire, 2014; 23(8):1097.

92. Marino E, Hernando C, Planelles R, Madrigal J, Guijarro M, Sebastián A. Forest fuel management for wildfire prevention in Spain: a quantitative SWOT analysis. International Journal of Wildland Fire, 2014; 23(3):373.

93. Lavoir a V, Ormeño E, Pasqualini V, Ferrat L, Greff S, Lecareux C, Vila B, Mévy JP, Fernandez C. Does prescribed burning affect leaf secondary metabolites in pine stands? Journal of chemical ecology, 2013; 39(3):398–412.

94. Valor T, González-Olabarria JR, Piqué M. Assessing the impact of prescribed burning on the growth of European pines. Forest Ecology and Management, 2015; 343:101–109.

95. Fernandes PM. Fire-smart management of forest landscapes in the Mediterranean basin under global change. Landscape and Urban Planning, 2013; 110:175–182.

96. Ager A a, Vaillant NM, Owens DE, Brittain S, Hamann J. Overview and Example Application of the Landscape Treatment Designer. Portland, OR: USDA Forest Service, Rocky Mountain Research Station; 2012. 11 p. Report No.: General Technical Report PNW-GTR-859

97. INSEE. Évolution de La Population Totale Au 1er Janvier 2014. France: Institut national de la statistique et des études économiques; 2014. Available at: http://www.insee.fr/fr/themes/tableau.asp?reg_id=6&ref_id=poptc02101

98. ISTAT. Popolazione Residente Al Primo Genaio 2014. Italy: Istituto Nazionale di Statistica; 2014. Available at: http://demo.istat.it/pop2014/index1.html

99. Promethée. Forest Fires Database for Mediterranean Area in France 2013. Available at: http://www.promethee.com/incendie